

ENVIRONMENTAL EFFECTS ON EVOLUTION OF CLUSTER GALAXIES IN A Λ CDM UNIVERSE

TAKASHI OKAMOTO

Yukawa Institute for Theoretical Physics, Kyoto Univ., Sakyo-ku, Kyoto 606-8502 Japan
tokamoto@yukawa.kyoto-u.ac.jp

AND

MASAHIRO NAGASHIMA

National Astronomical Observatory, Mitaka, Tokyo 181-8588, Japan
masa@th.nao.ac.jp

Submitted to The Astrophysical Journal

NAOJ-Th-AP2001, No.52

ABSTRACT

We investigate environmental effects on evolution of cluster galaxies under hierarchical structure formation scenario using combination of a dissipationless N -body simulation and a semi-analytic model of galaxy formation. The N -body simulation enables us to calculate orbits of galaxies in simulated clusters. Therefore we can include stripping of cold gas from the galactic disks by ram pressure from an ICM in our model. In this paper we consider galaxy mergers, stripping of diffuse hot gas from galactic halos as they infall into larger virialized objects, and ram-pressure stripping of cold gas from galactic disks. We find that observed color and star formation gradients in galaxy clusters are explained by the hot gas stripping as previous work has shown. Since the hot gas stripping sufficiently suppress star formation in clusters, the ram-pressure stripping of cold gas hardly affects the global properties of the cluster galaxies. We also examine whether the ram-pressure stripping can resolve the problem that the simulated clusters contain too few galaxies with intermediate bulge-to-disk ratio under the hierarchical galaxy formation. We, however, find that the ram-pressure stripping gives little change in morphologies of the cluster galaxies. It suggests that the additional processes other than major mergers and ram-pressure stripping, which affect the morphological evolution of disk-dominated galaxies, should be considered to reproduce the observed intermediate population in clusters.

Subject headings: galaxies: formation — galaxies: evolution — galaxies: clusters: general — galaxies: halos — galaxies: interactions

1. INTRODUCTION

Rich clusters of galaxies are the most suitable laboratory for studying how galaxy environments affect galaxy properties. The pioneering work by Butcher & Oemler (1978, 1984) has demonstrated that distant clusters contain much higher fraction of blue galaxies than nearby clusters. It has been also found that galaxy morphology is a function of its environment (Dressler 1980; Whitmore, Gilmore, & Jones 1993). The most recent advances have been made with the *Hubble Space Telescope*, which allows the morphology of distant galaxies to be directly compared with the properties of their nearby counter parts. Dressler et al. (1997) and Couch et al. (1998) have suggested that the predominant evolutionary effects are that the distant clusters have a substantial deficit of S0 systems compared with nearby clusters, and at lower luminosities they contain substantial Sc-Sd spirals, compared with the large population of dwarf spheroidals in present-day clusters. On the other hand, some recent studies (e.g. Abraham et al. 1996; van Dokkum et al. 1998; Balogh et al. 1999) have focused on observed trends in star formation rate (SFR) and morphology as a function of position within a cluster. These studies have shown that there is smooth transition from a blue, disk-dominated population of galaxies in the outskirts of clusters to a red, bulge-dominated population in the cluster cores.

Many authors have suggested that the predominance of red, early-type galaxies in local clusters is the result of mechanisms that suppress star formation in high-density environments. This

suppression makes galaxies within cluster cores redder and leads to a transformation of galaxy morphology. Comparison between the galaxy populations of local and distant clusters or those in cluster cores and outskirts provides a strong evidence for this scenario. This leads to a naive conclusion that the primary effect of the cluster environment is to transform luminous spiral galaxies into S0 galaxies through the suppression of their star formation.

Several mechanisms that may suppress the star formation and transform one morphological type into another have been proposed.

Interactions between galaxies are one possible process to promote morphological transformation. N -body simulations confirmed that major mergers between disk galaxies produce galaxies resembling ellipticals as merger remnants (e.g. Barnes 1996) and that accretion of small satellites onto their host spiral lead the morphology of the host spiral to S0 type (Walker, Mihos, & Hernquist 1996). The galaxy mergers trigger the *star burst*, therefore the cold gas contained in these galaxies are exhausted in a very short time. These processes then cause the truncation of the star formation. Although the bulge formation scenario by major mergers gives an excellent explanation both for colors (Kauffmann & Charlot 1998; Nagashima & Gouda 2001) and distribution of cluster ellipticals (Okamoto & Nagashima 2001; Diaferio et al. 2001), the observed S0 population cannot be reproduced only by major mergers (Okamoto & Nagashima 2001; Diaferio et al. 2001). In addition, the galaxy mergers are predominant effect mainly before massive cluster

formation, because, in clusters, the relative velocity of galaxies is too high for such mergers to be frequent (Ghigna et al. 1998; Okamoto & Habe 1999). Therefore the galaxy merger is hardly promising as a key mechanism behind the Butcher-Oemler effect. Moore et al. (1996) have examined the effects of rapid gravitational encounters between galaxies. This mechanism has been called *galaxy harassment* and is highly effective at transforming fainter Sc-Sd galaxies to dSphs. While the galaxy harassment can account for the observed evolution of faint galaxies in clusters, the concentrated potentials of luminous Sa-Sb galaxies help to maintain their stability (Moore et al. 1999), although their disks are substantially thickened.

The second mechanism is the truncation of star formation through the removal of the diffuse hot gas reservoir that is confined in galactic dark halos and surrounds galaxies (Larson, Tinsley, & Caldwell 1980). In clusters, any hot diffuse material originally trapped in the potential of the galactic halos becomes part of the overall intracluster medium (ICM). A galaxy whose hot gas reservoir is removed slowly exhausts its cold gas in a few gigayears (e.g. Gallagher, Bushouse, & Hunter 1989), since there is no supply of the fresh gas from the surrounding hot gas. This process is an important ingredient in the success of semi-analytic models, which have been shown to reproduce observed global cluster properties such as the morphological composition and the blue galaxy fraction (e.g. Baugh, Cole, & Frenk 1996; Kauffmann 1996). Although such slow truncation after infalling into larger virialized halos explains the observed star formation gradients in clusters (Balogh, Navarro, & Morris 2000) and the color evolution of cluster galaxies (Kodama & Bower 2001), the lack of the population of intermediate bulge-to-disk ratios cannot be solved even by including this mechanism into the galaxy formation model (Diaferio et al. 2001).

The other mechanism is the ram-pressure stripping of the cold gas from galactic disks (Gunn & Gott 1972). As a galaxy orbits through a cluster, it undergoes a ram pressure from the ICM. When the ram-pressure is greater than the binding force, the cold gas will be stripped in $\sim 10^7$ yr (Abadi, Moore, & Bower 1999). Fujita & Nagashima (1999) have suggested that the ram-pressure stripping increases *B*-band bulge-to-disk luminosity ratios of the disk galaxies owing to the rapid suppression of the star formation in the disk component, and consequently Sb galaxies change their morphology into S0 galaxies. Thus, there is a possibility that the ram pressure stripping solve the deficient intermediate population in clusters under the hierarchical galaxy formation.

In this study we investigate how these mechanisms affect colors and morphologies of the cluster galaxies with a special interest in the effects of the ram-pressure stripping. For this purpose, the fully numerical simulations are still too expensive and have a lot of difficulty in handling *subgrid* physics, e.g. gas cooling, star formation, supernova feedback, chemical evolution and so on, though recent work is beginning to achieve some notable successes for the distribution of galaxy populations (e.g. Steinmetz & Müller 1995; Weinberg, Hernquist, & Katz 1997; Blanton et al. 1999; Katz, Hernquist, & Weinberg 1999; Pearce et al. 1999; Cen & Ostriker 2000).

Alternative method to study the evolution of galaxy population is the semi-analytic modeling of galaxy formation (e.g. Kauffmann, White, & Guiderdoni 1993; Cole et al. 1994; Somerville & Primack 1999; Cole et al. 2000; Nagashima et al. 2001), which follows the collapse and merging of dark halos by using a probabilistic method on the mass distribution based

upon an extension of the Press-Schechter formalism (Press & Schechter 1972; Bond et al. 1991; Bower 1991; Lacey & Cole 1993) and in which the subgrid physics is incorporated with the merging histories of dark matter halos assuming simple scaling laws.

As a natural expansion of this approach, hybrid methods of cosmological *N*-body simulations and the phenomenological model of galaxy formation used in the semi-analytic techniques have been developed (Roukema et al. 1997; Kauffmann et al. 1999; Benson et al. 2000). In order to obtain the spatial and velocity distribution of the galaxies and to treat the mergers between galaxies in the cluster environment, several authors have adapted the refinements of hybrid methods, which traces the merging histories of substructures within virialized halos (Okamoto & Nagashima 2001; Springel et al. 2000).

Since this method enables us to calculate orbits of galaxies in clusters, we can incorporate the ram-pressure stripping process in our model. Using this method we here explore effects of two kinds of gas stripping, i.e. the stripping of diffuse hot gas from galactic halos and the ram-pressure stripping of cold gas from galactic disks, on properties of cluster galaxies as a function of projected clustercentric distance.

We compare our simulated cluster at $z = 0.2$ to an observed sample that is constructed by superposing 7 low redshift CNOC1 (Yee, Ellingson, & Carlberg 1996) clusters ($0.18 < z < 0.3$). To compare our results with the observations, we rescale our simulated cluster and the CNOC1 clusters by R_{200} which is the radius of the sphere centered on the center of a cluster and whose density is 200 times the critical density of the universe at a given redshift.

In §2, we describe an outline of the galaxy formation model used here and we show the characteristics of our model in §3. Results on the luminosity functions, star formation gradients, color gradients, and morphological gradients are presented in §4. These results are discussed in §5.

2. MODEL

We examine the evolution of cluster galaxies in a Λ CDM univers ($\Omega_0 = 0.3$, $\Lambda_0 = 0.7$, $h \equiv H_0/100 \text{ km s}^{-1} \text{ Mpc}^{-1} = 0.7$, $\sigma_8 = 1$). The baryon density is set to $\Omega_b = 0.015h^{-2}$.

The outline of the procedures of galaxy formation is as follows. At first, the merging paths of dark halos are realized by a cosmological *N*-body simulation. At this stage, it is determined for each halo whether it is a central halo of its virialized host halo or it is a substructure of its host. Next, in each merging path, evolution of the baryonic components, namely, gas cooling, star formation, supernova feedback, and chemical evolution, are calculated based on an ordinary semi-analytic galaxy formation model. We refer a system consisting of the stars and cold gas as a *galaxy*. When two or more galactic halos merge together, we estimate merging time-scale based on dynamical friction time-scale. As merging of galaxies occurs, we change the morphology of the merger remnant according to the type of the merger. Finally, we calculate the luminosity and color of each galaxy based on the stellar populations that compose the galaxy.

2.1. Simulations

We first describe two simulations used in this paper and their specific purpose. These simulations are the same as the simulations by Okamoto & Habe (1999, 2000) except for the background cosmology.

For a main simulation, we adopt the constrained random field method to generate the initial density perturbation field in which a rich cluster is formed at the center of a simulation sphere of radius $22.5 h^{-1}$ Mpc (Hoffman & Ribak 1991). The constraint that we impose is the 3σ peak with the 8 Mpc Gaussian smoothed density field at the center of the simulation sphere. We refer this simulation as the *cluster simulation*.

Another simulation represents an average piece of the universe corresponding to the *field* environment within a sphere of radius $20 h^{-1}$ Mpc without any constraints. We use this simulation to normalize the parameters in our galaxy formation model and to compare the galaxy population to that in the cluster simulation.

To get sufficient resolution with a relatively small number of particles we use the multimass initial condition for each simulation. In the field simulation, we put the high-resolution particles in the sphere of radius $10 h^{-1}$ Mpc and in the remaining region we put the low-resolution particles as boundary particles. On the other hand, we adopt the resimulation technique for the cluster simulation (Okamoto & Habe 1999). That is, first, only long-wavelength components are used for the realization of the initial perturbation in the simulation sphere using $\sim 10^5$ particles, and then we perform a simulation with these low-resolution particles. After this procedure, we tag the particles that are inside the sphere of radius 3 Mpc centered on the cluster center at $z = 0$. Next we go back to the initial redshift, and then we divide the tagged particles according to the density perturbation that is produced by additional shorter wavelength components. As a result, the number of the high-resolution particles becomes $\sim 10^6$. We adopt same mass and softening length of a high-resolution particle in each simulation. Our analyses are operated only for these high-resolution particles.

The overall parameters and mass of the most massive virialized object in each simulation at $z = 0$ are listed in Table 1.

2.2. Halo Identification and Construction of Merger Trees

The method to create merging history trees of dark halos is basically the same as Okamoto & Habe (2000), while we make some improvement based on Springel et al. (2000).

To construct the merger trees we identify virialized halos and their substructures at 34 time-steps during $z = 20$ and $z = 0$. This procedure is as follows.

At each time-step, we calculate density field by smoothing each particle using the SPH-like method with neighboring 64 particles. At a given redshift, particles with local densities greater than one-third of the virial density at that epoch are tagged. We then operate the friends-of-friends (FOF) grouping algorithm (Davis et al. 1985) on the tagged particles. The linking length is defined as $b\bar{l}$, where \bar{l} is the mean particle separation, and the parameter b is a function of redshift. Its value is given by

$$b = \left(\frac{1}{2} \frac{\rho_{\text{vir}}}{\bar{\rho}} \right)^{-\frac{1}{3}}, \quad (1)$$

where ρ_{vir} is the virial density calculated by spherical collapse model at a given redshift and $\bar{\rho}$ is the background density of the universe. Eq. (1) gives ~ 0.2 when we assume 200 as the virial overdensity, which is often used in the case of the critical universe. We identify the groups that contain more than 10 particles as the virialized objects. We call these halos *FOF-halos*.

Next, we divide these FOF-halos into substructures according to their density peaks. For this purpose, we use SKID algorithm (Governato et al. 1997) as a substructure finder. The

particles contained in the FOF-halos are moved along the density gradients to the local density maxima. At each density peak, the localized particles are grouped. After we remove the gravitationally unbound particles in each group, we identify the groups that contain more than 10 particles as substructures. We call these groups *SKID-halos*. A SKID-halo that contains the most bound particle of each host FOF-halo is defined as a central SKID-halo and its properties are replaced by those of the host FOF-halo. In Fig. 1, we show the density map of the cluster at $z = 0$ and the particles in the FOF-halos and the SKID halos.

The merger tree of each SKID-halo is constructed by the method in Okamoto & Habe (2000). Note that we trace halo-stripped galaxies as well as the SKID halos using the most bound particle in a SKID-halo as a tracer particle (see Okamoto & Habe 1999, 2000).

Finally, we remove newly formed non-central SKID-halos and their descendants from the merger trees so that SKID-halos are always born as central SKID-halos.

2.3. Galaxy Formation Model

The following prescriptions are almost the same as the model in Okamoto & Nagashima (2001).

2.3.1. Gas Cooling

For simplicity, a dark halo is modeled as an isothermal sphere whose mass and circular velocity are taken from the N -body data. The source of the diffuse gas in a virialized halo is hot gas contained in its progenitor halos and in the accreting matter. The baryon fraction of the accreting matter is defined as $f_b = \Omega_b/\Omega_0$. We assume that the hot gas has the distribution that parallels to that of the dark matter with the virial temperature of the halo.

The cooling time-scale τ_{cool} is obtained as a function of the radius from the hot gas density profile, the temperature of the hot gas, and the cooling function $\Lambda(T)$ as follows,

$$\tau_{\text{cool}} = \frac{2}{3} \frac{\rho(r)}{\mu m_p n_e^2 \Lambda(T)}, \quad (2)$$

where μm_p is the mean molecular weight, $n_e(r)$ is the electron number density at the radius r , and k is the Boltzmann constant. Using the zero-metallicity and solar-metallicity cooling functions given by Sutherland & Dopita (1993), the cooling efficiency depending on the metallicity of the gas is calculated by interpolation and extrapolation.

We assume that diffuse hot gas contained in a halo is reheated by shock to the virial temperature of the halo when the halo mass becomes more than double of the forming or last reheating time (Somerville & Primack 1999). The cooling radius, r_{cool} , is defined as a radius at which the cooling time-scale, τ_{cool} , equals to the elapsed time from last reheating time of the halo. The hot gas that distributes between $r_{\text{cool}}(t)$ and $r_{\text{cool}}(t + \Delta t)$ is cooled and added to the cold gas reservoir of the galaxy during the time-step, Δt .

2.3.2. Star Formation and Supernova Feedback

In this paper, the star formation in a disk is described by the following simple law,

$$\dot{M}_* = \frac{M_{\text{cold}}}{\tau_*}, \quad (3)$$

where eq.(3) denotes the rate of stars newly formed and τ_* is the star formation time-scale. It means that the cold gas in a disk is almost consumed in τ_* if there is not any supply of the fresh gas. When the star formation time-scale is a function of redshift as in the case of $\tau_* \propto \tau_{\text{dyn}}$, where τ_{dyn} is the dynamical time of a galaxy, the observed properties of the high redshift galaxies cannot be reproduced (Kauffmann & Haehnelt 2000; Somerville, Primack, & Faber 2001; Nagashima et al. 2001). We then adopt the description by Cole et al. (1994),

$$\tau_* = \tau_*^0 \left(\frac{V_c}{300 \text{ km s}^{-1}} \right)^{\alpha_*}, \quad (4)$$

where τ_*^0 and α_* are free parameters. The first, τ_*^0 , determines the star formation time-scale in the galaxy with $V_c = 300 \text{ km s}^{-1}$, while the second, α_* , determines how this time-scale varies with circular velocity.

When stars form, massive stars with short lifetime explode and heat up the surrounding cold gas. The number of super novae per solar mass of newly formed stars is $\eta_{\text{SN}} \simeq 7 \times 10^{-3} M_{\odot}^{-1}$ for the Salpeter's (1955) initial mass function (IMF). The energy from a supernovae, E_{SN} , is about 10^{51} erg. When a fraction ϵ of the released energy is used to heat up surrounding cold gas, the amount of the reheated gas during Δt is evaluated as

$$\Delta M_{\text{reheat}} = \epsilon \frac{4 \dot{M}_* \eta_{\text{SN}} E_{\text{SN}}}{5 V_c^2} \Delta t. \quad (5)$$

This feedback process has many uncertainties actually, and therefore we adopt a simple description by Cole et al. (1994),

$$\Delta M_{\text{reheat}} = \left(\frac{V_c}{V_{\text{hot}}} \right)^{-\alpha_{\text{hot}}} \dot{M}_* \Delta t, \quad (6)$$

where V_{hot} and α_{hot} are free parameters. Eq.(5), which is adopted by Kauffmann, White, & Guiderdoni (1993), corresponds to $\alpha_{\text{hot}} = 2.0$ when ϵ is independent of V_c , and Cole et al. (2000) also use this value in their reference model. Therefore we here adopt $\alpha_{\text{hot}} = 2.0$, and then we will adjust V_{hot} to reproduce the observed luminosity functions of the local galaxies. We assume that the heated gas by the feedback returns to the halo when the mass of the host FOF-halo is doubled, i.e. next reheating time (Cole et al. 1994).

2.3.3. Mergers of Galaxies and Bulge Formation

When two or more SKID-halos merge together, we identify a central galaxy of the largest progenitor as a central galaxy of the new common SKID-halo. Note that galaxies must be born as centrals. Other galaxies are identified as satellites. These satellites merge with the central galaxy in the dynamical friction time-scale,

$$\tau_{\text{mrg}} = \frac{1}{2} \frac{f(\epsilon)}{C} \frac{V_c r_{\text{halo}}^2}{G M_{\text{sat}} \ln \Lambda_C}, \quad (7)$$

where r_{halo} and V_c are the radius and circular velocity of the new common halo, respectively, M_{sat} is the total mass of the halo to which the satellite belonged as the central galaxy or the mass of the galaxy composed by stars and cold gas in the case that the satellite was the halo-stripped galaxy, and $\ln \Lambda_C$ is the Coulomb logarithm, which is approximated as $\simeq \ln(1 + M_{\text{halo}}^2 / M_{\text{sat}}^2)$ (Somerville & Primack 1999). The function $f(\epsilon)$ describes the dependence of the orbital decay on the eccentricity of the orbit, expressed in terms of $\epsilon = J/J_c(E)$, where $J_c(E)$ is the angular momentum of a circular orbit with the same energy as the satellite. This function is well approximated by $f(\epsilon) \simeq \epsilon^{0.78}$, for $\epsilon > 0.02$ (Lacey & Cole 1993). C is

a constant with value $\simeq 0.43$. For $f(\epsilon)$, we adopt the average value, $\langle f(\epsilon) \rangle \simeq 0.5$, computed by Tormen (1997) according to Kauffmann et al. (1999). When mass of a SKID-halo becomes more than double of that at its forming epoch, we recalculate this time-scale because orbits of satellites may be violently disturbed in such a case similar to the reheating of hot gas in FOF-halos.

When a satellite galaxy merges with a central galaxy and the mass ratio of the satellite to the central galaxy is larger than f_{bulge} , we regard this merger as a major merger, and then all stars of the satellite and disk stars of the central galaxy are incorporated with the bulge of the central galaxy. At the same time, cold gas contained in both galaxies is consumed to form bulge stars by starburst with the same feedback law as in the disk star formation.

If the mass ratio does not exceed the value of the parameter, f_{bulge} , the merger is classified as minor. In the minor merger, the disk of the central galaxy is preserved, no starburst takes place, and the stars from the satellites are added to the bulge of the central galaxy.

In this paper, we adopt $f_{\text{bulge}} = 0.2$ that was used for the low-density universe by Okamoto & Nagashima (2001). We confirmed that our results hardly depend on f_{bulge} , since our morphological classification based on bulge-to-disk luminosity ratio is normalized to reproduce the observed morphological composition in the field.

2.3.4. Chemical Evolution

Chemical evolution is treated in almost the same way as described in Kauffmann & Charlot (1998) and Nagashima & Gouda (2001). The instantaneous recycling approximation is adopted. The amount of metals ejected from evolved stars is characterized by y , which is heavy element yield for each generation of stars. The gas fraction returned by evolved stars is 0.25 in this paper. Simultaneously, the supernovae heat up the surrounding cold gas, then metals contained in the cold gas are also returned to the hot gas.

2.3.5. Stellar Population Synthesis and Identification of Morphologies

In order to compare our results with observations directly, stellar population synthesis model that is combined with star formation histories of galaxies estimated by our model must be considered. We use a simple stellar population given by Kodama & Arimoto (1997). The IMF that we adopt is the Salpeter type with a slope of 1.35, and the mass range is $0.1 M_{\odot} \sim 60 M_{\odot}$. The luminosity of disks and bulges is given by this model in each pass-band according to the metallicities and ages of stars. Note that in this paper we do not attempt to model the effects of dust. Although these effects can be substantial in gas rich late-type galaxies and would affect our results (Somerville & Primack 1999; Cole et al. 2000), we here concentrate on the effects of gas stripping.

In §2.3.3, we divided the stellar component into disk and bulge components. In the previous semianalytic studies, morphology of each galaxies have been determined by the B -band bulge-to-disk luminosity ratio (B/D). Simien & de Vaucouleurs (1986) showed that the Hubble types T of galaxies correlated with B/D by following relation,

$$\langle \Delta M \rangle = 0.324(T+5) - 0.054(T+5)^2 + 0.0047(T+5)^3, \quad (8)$$

where $\Delta M \equiv M_B^{\text{bulge}} - M_B^{\text{total}}$. In this paper we use this relation to assign the Hubble type to our model galaxies. However, this

relation has significant scatter (Baugh, Cole, & Frenk 1996), therefore we prefer direct comparison of B/D of model galaxies with B/D of observed galaxies as we will describe in §4.4.

2.3.6. Stripping of Diffuse Hot Gas

We include stripping of diffuse hot gas in galactic halos into our modeling as follows. When a FOF-halo contains more than two SKID-halos, we identify the central SKID-halo and properties of this central SKID-halo are replaced with those of the host FOF-halo as we mentioned in §2.2. The hot gas contained in the non-central SKID-halos are simply added to hot gas reservoir of the host FOF-halo (i.e. the central SKID-halo), therefore only the central galaxy in the central SKID-halo can be supplied with the fresh cold gas by radiative cooling. This process has already been included in the previous semi-analytic studies based on the extended Press-Schechter model or combination with N -body simulations and led significant success (e.g. Baugh, Cole, & Frenk 1996; Kauffmann & Charlot 1998; Diaferio et al. 2001).

2.3.7. Ram-pressure Stripping of Cold Gas Disk

By following simple method, we estimate stripping effects of cold gas contained in galactic disks by ram-pressure from an ICM.

In order to estimate the strength of the ram-pressure, we need to know orbits of cluster galaxies. For this purpose, we assume that the clusters have NFW-type of density distribution (Navarro, Frenk, & White 1997, hereafter NFW) and then we fit the density profile of the main cluster (i.e. the most massive virialized object) at each time-step of the merging history by the NFW profile,

$$\rho(r) = \frac{\rho_0}{(r/r_s)(1+r/r_s)^2}, \quad (9)$$

where ρ_0 and r_s are fitting parameters. Once we fit the density profile of a cluster, we can calculate the potential energy as a function of the distance from the cluster center,

$$\Psi(r) = -4\pi r_s^2 G \rho_0 \frac{\ln(1+r/r_s)}{r/r_s} + \frac{1}{2} \Lambda_0 r^2, \quad (10)$$

where r is the distance from the cluster center. Then we calculate the orbits of the galaxies within $2R_{\text{vir}}$ from the center of the main cluster using their positions and relative velocities to the cluster.

We assume that ingoing galaxies are stripped their pericentric positions during the time-step of its merger tree and outgoing galaxies are stripped at their present positions. Since some galaxies have much longer orbiting periods than the time-step of their merger trees (~ 0.5 Gyr), we may overestimate the stripping effect for such galaxies. It should be noted that, in this paper, we examine only the case that the ram-pressure stripping is quite efficient.

The ram-pressure from the ICM is

$$P_{\text{ram}} = \rho_{\text{ICM}} v_{\text{gal}}^2, \quad (11)$$

where ρ_{ICM} is the density of the ICM and v_{gal} is the velocity of a galaxy relative to the ICM. We suppose that the ICM distributes parallel to the dark matter for simplicity. The density of the ICM is obtained as $f_b \rho_{\text{DM}}(r)$, where $\rho_{\text{DM}}(r)$ is taken from the NFW fit. We also attempted the ICM distribution that has the Coma-like core, i.e. $\rho_c = 7.98 \times 10^{-27} h^{\frac{1}{2}} \text{ g cm}^{-3}$ (Briel, Henry, & Böhringer 1992), and then we found that results are almost identical. Therefore we show only the results in the case of the

ICM distribution parallelized to dark matter. For the cold gas, the restoring force per unit area due to the gravity of the galactic disk is given by

$$F_{\text{grav,cold}} = 2\pi G \Sigma_{*,\text{disk}} \Sigma_{\text{cold}}, \quad (12)$$

where $\Sigma_{*,\text{disk}}$ is surface density of the stellar disk and Σ_{cold} is that of the cold gas (Gunn & Gott 1972). We calculate $\Sigma_{*,\text{disk}}$ according to the relation $\Sigma_{*,\text{disk}} = (2\pi G)^{-1} V_c^2 R^{-1}$ (Binney & Tremaine 1987), where V_c is the circular velocity of the galaxy and R is the radius of the disk. We use the half mass radius of the disk as R . Assuming $\Sigma_{\text{cold}} \propto \Sigma_{*,\text{disk}}$, the surface density of the cold gas can be given by $\Sigma_{\text{cold}} = (M_{\text{cold}}/M_{*,\text{disk}}) \Sigma_{*,\text{disk}}$.

Because we consider the most efficient case of the ram-pressure stripping, all of the cold gas is stripped when

$$P_{\text{ram}} > F_{\text{grav}}. \quad (13)$$

The stripped cold gas is mixed with the hot gas of the host FOF-halo.

3. MODEL SETS

In this paper we investigate following three models to clarify effects of the gas stripping.

In the first model, we consider only the hot gas stripping for the galaxies in the cluster simulation. Since this treatment is the same as the traditional semi-analytic models, we call this model the *standard* model. In the second model, we include the ram-pressure stripping of the cold gas besides the hot gas stripping. We refer this model as the *ram-pressure* model. By comparison of these two models we show the effects of the ram-pressure stripping. The final model is the same as the standard model but for the field simulation. We call this model the *field* model and use to specify the parameters in our galaxy formation model so that the properties of the galaxies in this model reproduce the observational properties of the local galaxies. Because the most of bright galaxies in the field model are the central galaxies of the central SKID-halos, influence of the hot gas stripping is probably negligible for such galaxies. Therefore we can see the effects of the hot gas stripping by comparing this model with the standard model for the cluster simulation.

3.1. Parameter setting

In this subsection we show characteristics of our reference model and how the model parameters affect properties of galaxies. The values of the parameters used in the reference model are listed in Table 2.

As shown in Cole et al. (2000), luminosity function has strong dependence only on the feedback parameters, V_{hot} and α_{hot} . First, we examine influence of the model parameters upon luminosity functions of the galaxies in the field model. In Fig. 2, we show the observed B -band luminosity functions from APM (Lovely et al. 1992), ESP (Zucca et al. 1997), UKST (Ratcliffe et al. 1998), and 2dF (Folkes et al. 1999) and the model luminosity functions at $z = 0$. The reference model (solid line) and the model that is changed the star formation parameters, $\tau_*^0 = 1.0$ Gyr and $\alpha_* = -2.0$ (dotted line), show similar luminosity functions, although there is small difference at bright end because of the small simulation volume of the field simulation. It is confirmed that the star formation parameters hardly affect the luminosity functions and this result is consistent with Cole et al. (2000). It is also found that the model luminosity function is smaller than the observations at the intermediate luminosity range and the slope at faint-end is steeper than

those. This difference may cancel out if random collisions between satellite galaxies by the mean free time-scale are considered (Somerville & Primack 1999) or if we use a higher resolution simulation that enables us to identify dark halos of small satellite galaxies (Springel et al. 2000). The luminosity function with strong feedback, $V_{\text{hot}} = 300 \text{ km s}^{-1}$ is represented by dashed line. The strong feedback decreases the number of faint galaxies. We have confirmed that the choice of these parameters does not change our conclusion if we choose these parameters in order to reproduce the observed cold gas content in the local late-type galaxies, as we will describe in the following paragraph.

When examining the effects of gas stripping, the most important normalization of our model is specifying the model parameters so that they reproduce the observed cold gas fraction in galaxies that reside in the environment where the stripping effects are negligible. The cold gas content of galaxies are strongly affected by the star formation parameters, τ_*^0 and α_* (Cole et al. 2000). Fig. 3 shows how the amount of cold gas in spiral and irregular galaxies depends on galaxy luminosity. The observational data are taken from the H_I observation by Huchtmeier & Richter (1988), which come from a complete sample of the galaxies with morphological type $T \geq 1$. We classify our galaxy according to eq. (8) and choose the galaxy with $T \geq 1$. In the upper panel we show the cold hydrogen fraction of the field galaxies with the reference model (solid line). It is found that this model reproduces the observation well. In the lower panel we show the models with $\tau_*^0 = 1.0 \text{ Gyr}$ (solid line) and $\alpha_* = 0.0$ (dotted line). In the case of $\alpha_* = 0$ the star formation time-scale is a constant for all galaxies. In this case, the faint galaxies in the model typically contain much less cold gas than the observation (see also Cole et al. 2000). The model with $\tau_*^0 = 1 \text{ Gyr}$ shows the effect of varying τ_*^0 . The short star formation time-scale reduces the amount of the cold gas of the galaxies in all luminosity range.

It should be noted that we neglect the H_2 content, therefore we underestimate the amount of the cold hydrogen in the observed galaxies. However such small deference probably does not affect our results and may be absorbed in errors.

The chemical yield in the reference model is specified so that the color-magnitude relations (CMRs) of cluster ellipticals at $z=0$ in our standard model reproduces the observational CMRs. We here identify the model galaxies with $T < -2.5$ according to eq. (8) as ellipticals. In Fig. 4, we show the observational CMRs (Bower, Lucy, & Ellis 1992) applied aperture correction (solid line, Kodama et al. 1998) and the CMRs of the model ellipticals within the cluster core ($r < 0.5h^{-1} \text{ Mpc}$). We plot the CMRs for the reference model ($y = 3.0Z_{\odot}$) in the left panels, and CMRs for the model with $y = 2.0Z_{\odot}$ in the right panels. We find that the value of the chemical yield is directly reflected in the CMRs of cluster ellipticals and large yield such as $y = 3.0Z_{\odot}$ is needed to reproduce the observations in our model. With the reference model, metallicity of the ICM at $z=0$ becomes $\sim 0.37Z_{\odot}$.

In this paper we investigate effects of gas stripping on cluster galaxies with the reference model.

4. RESULTS

4.1. Global Properties

Before we investigate radial gradients, we show global properties of our model galaxies.

In Fig. 5, we show B -band luminosity functions of cluster

galaxies in the standard and ram-pressure models at $z=0$. We also show the observed luminosity function in the Virgo cluster (Sandage, Binggeli, & Tammann 1985). We cannot find significant difference between these two models. Each model luminosity function reproduces the observed one well, although the number of the galaxies in the intermediate luminosity range is slightly smaller than the observation similar to the luminosity functions in the field model.

To see effects of gas stripping on colors of galaxies, CMRs for all types of galaxies in the field model and galaxies within cluster cores ($r < 0.5h^{-1} \text{ Mpc}$) in the standard and ram-pressure models are shown in Fig. 6. In all models we classify the galaxies with $T < 0.92$ according to eq. (8) as early-type galaxies (diamonds) and others as late-type galaxies (pluses). In the standard model, the blue population seen in the field model is vanished, and then the galaxies distribute within $\pm 2 \text{ mag}$ from the CMR for the observed cluster ellipticals (solid line, Bower, Lucy, & Ellis 1992) as observed in Coma cluster (Terlevich, Caldwell, & Bower 2001). This is probably caused by the hot gas stripping in the standard model and earlier formation epochs of galactic halos in the cluster environment (Gottlöber, Klypin, & Kravtsov 2001). Although, in the ram-pressure model, the CMR becomes redder at the faint end than that in the standard model, they are quite similar and both well reproduce the observation.

It is also found that the CMR for early-type galaxies in the field model have almost the same slope as that for cluster ellipticals, while it is bluer than those for the cluster population and has large scatter at faint end. It is because that field ellipticals has the same metallicity-magnitude relation as cluster ellipticals (Kauffmann & Charlot 1998) and the stars in the field ellipticals are younger than those in the cluster ellipticals (Baugh, Cole, & Frenk 1996; Kauffmann & Charlot 1998). In our case, the cluster ellipticals in the standard model have uniform ages ($\sim 10 \text{ Gyr}$), while the ages of the ellipticals in the field model widely distribute from 1 Gyr to 10 Gyr. The younger ages of field early-type galaxies are explained by the fact that in the field environment merger rate has a peak at lower redshift than in the cluster forming regions (Okamoto & Habe 2000; Gottlöber, Klypin, & Kravtsov 2001) and collapse epochs of dark halos in the field environment are also later than in the cluster forming regions (Gottlöber, Klypin, & Kravtsov 2001). The merger rate in the cluster forming regions quickly decreases after the peak epoch, and then the merger rate in the field environment become larger than that in the cluster forming regions at $z < 2$ (Okamoto & Habe 1999; Gottlöber, Klypin, & Kravtsov 2001).

In the next subsection we will explore why the standard and ram-pressure models produce almost the same galaxy populations, and we will make detailed analysis on colors and morphologies in the following subsections.

4.2. SFR Gradients

Recently, many authors have analyzed radial trends in SFR (Balogh et al. 1998; Balogh et al. 1999; Ellingson et al. 2001) of galaxies in the CNOC1 sample (Yee, Ellingson, & Carlberg 1996). In order to clarify effects of the ram-pressure on SFRs, we compare the SFRs in the standard model with those in the ram-pressure model as a function of projected radius.

In Fig. 6 we show the observed SFR distribution taken from Diaferio et al. (2001). The galaxies brighter than $M_R = -20.5$ are selected assuming the same cosmology as our simulations.

In this figure we show the low redshift sample of Diaferio et al. (2001), that is, the data were constructed by superposing 7 CNOC1 clusters at the redshift range between $0.18 < z < 0.3$. Hereafter, we refer this superposing sample as the *CNOC sample* in this paper. The details are given in Diaferio et al. (2001) and references therein. According to Diaferio et al. (2001) we regard this superposed data as the data from clusters at $z \sim 0.2$. We show the relative SFRs, i. e. they are normalized by the field median value obtained from the same redshift range, because the observed SFRs determined by W_{OII} have a lot of uncertainties. We also show SFRs of our cluster galaxies with $M_R < -20.5$ at $z = 0.2$. In this luminosity range, most of our galaxies have their SKID-halos. Both of the observational and simulation data, we exclude the brightest cluster galaxies because they often have quite different properties from other cluster galaxies.

It is found that the both models reproduce the observed SFR distribution of cluster galaxies relative to the field quite well. It is also found that, inside the cluster virial radius, the median SFR in the ram-pressure model is lower than that in the standard model. Although we can see such effect by the ram-pressure stripping in the SFR distribution, the difference between two models is very small and it cannot be distinguished observationally, because, only by the hot gas stripping, the SFRs of the cluster galaxies are sufficiently suppressed and they become almost 0 near the cluster center. This result is consistent with the previous studies that have suggested that the slow truncation of the star formation in clusters, which is expected in the case of the hot gas stripping, gives good explanation of the observed SFR gradients (Balogh, Navarro, & Morris 2000; Diaferio et al. 2001).

Since the hot gas stripping is very efficient, there is little cold gas in a disk when the cold gas is stripped by the ram-pressure. It is the reason why the models with and without the ram-pressure stripping produce the similar galaxy populations.

4.3. Color Gradients

Color of a galaxy reflects the SFR of the galaxy and is more reliable observable than the SFR. It has been known that galaxies in inner regions of clusters are redder than those in outer region (Butcher & Oemler 1984). Recent observations have confirmed the existence of the color gradients, and besides, it continues to large radii beyond the virial radii ($\sim 2R_{200}$) (Abraham et al. 1996; Carlberg et al. 1997).

In Fig. 7 we show the $B-V$ colors of the cluster galaxies as a function of the projected radius at $z = 0.2$. As the observational counterpart, we use the same sample that we used for the SFR gradients and the data are taken from Diaferio et al. (2001). That is, we choose the galaxies brighter than $M_R = -20.5$ again.

Both models reproduce the observed trend quite well. In the ram-pressure model the colors of the galaxies inside R_{200} become redder than the galaxies in the standard model. It directly reflects the suppression of the star formation by the ram-pressure stripping, which is seen in Fig. 6. However, the difference between these two models is not significant, because the cluster galaxies are sufficiently reddened only by the hot gas stripping compared with the field population.

The colors of the galaxies in each model are slightly redder than those of the CNOC sample. It is partly explained by the fact that our cluster samples are less contaminated by the field population than the observations, because we only calculated the small region around the cluster as we mentioned in §2.1.

4.4. Morphological Gradients

It is well established that galaxy morphology varies with a density of neighboring galaxies (morphology-density relation; Dressler 1980) or a clustercentric distance (morphology-radius relation; Whitmore, Gilmore, & Jones 1993) in nearby clusters. Whitmore, Gilmore, & Jones (1993) have found that if they normalize the clustercentric distance by a characteristic radius of each cluster, the morphology-radius relation becomes universal and independent of the richness of the clusters.

Recently, some authors have studied the morphology-density or morphology-radius relations by using hybrid method of N -body simulations and semi-analytic models (Okamoto & Nagashima 2001; Diaferio et al. 2001; Springel et al. 2000). All these papers conclude that the morphological evolution only by major mergers cannot explain the S0 or intermediate populations in clusters and additional processes are required to understand this population.

One possible process is the ram-pressure stripping of the cold gas in a galactic disk (Gunn & Gott 1972; Fujita & Nagashima 1999). According to Fujita & Nagashima (1999), at a central part of a cluster, the SFR of the disk component rapidly drops owing to the ram-pressure stripping, and then the galaxy becomes red and the disk becomes dark. They have suggested that a Sb galaxy is turned into a S0 galaxy as a result of the ram-pressure stripping.

We here examine this hypothesis by comparing our galaxy populations in the ram-pressure model with those in the standard model and the CNOC sample. Since we do not have any information about galaxy morphology in our models except for bulge-to-disk luminosity ratios, we classify the galaxies only by the bulge-to-disk luminosity ratios both in our models and the CNOC sample. According to Balogh et al. (1998), we classify our sample into three classes: a bulge-dominated class, a disk-dominated class, and an intermediate class. In CNOC sample, Diaferio et al. (2001) have split the galaxy population based on the r -band bulge-to-total luminosity ratios (B/T), and then galaxies with $B/T > 0.7$ are identified as bulge-dominated galaxies, $B/T < 0.4$ as disk-dominated galaxies, and $0.4 < B/T < 0.7$ as intermediate galaxies. We classify our model galaxies based on the B -band B/T . The boundaries between the morphological classes are chosen so that the morphological fractions in the field model match the fractions of the field galaxies in the CNOC sample. As a result, the galaxies with B -band $B/T > 0.4$ are identified as bulge-dominated galaxies, $B/T < 0.25$ as disk-dominated galaxies, and $0.25 < B/T < 0.4$ as intermediate galaxies. The morphological fractions of field galaxies with $M_R < -20.5$ are shown in the right of the top panel and middle panel of Fig. 8 for the CNOC sample and the standard model, respectively.

The fractions of galaxies with $M_R < -20.5$ in each class as a function of projected clustercentric radius are shown in Fig. 8. In the top, middle, and bottom panels, we show the fractions in the CNOC sample, standard model, and ram-pressure model, respectively. By comparison of the CNOC sample with the standard model, it is found that the bulge-dominated fraction in our model agrees with the observation within the errors, while the intermediate fraction in our model is much smaller than observed one. This problem has been indicated as a shortcoming of the major merger induced morphological evolution model (Okamoto & Nagashima 2001; Diaferio et al. 2001). When we consider the ram-pressure stripping, the bulge-dominated and intermediate fractions are increased in the innermost two bins

and show better agreement with the observation. This increase is, however, quite small, and then the deficient of the intermediate galaxies is still significant.

This result is naturally expected from the fact that the SFRs of our cluster galaxies are sufficiently suppressed solely by the hot gas stripping and then the effect of the ram-pressure stripping becomes small (Fig. 6).

One might think that the shortage of the intermediate population is an artifact by our morphological classification. We then adapt wider B/T range for the intermediate galaxies. To solve the problem of too large disk-dominated fraction and too small intermediate fraction, we identify the galaxies with $0.15 < B/T < 0.4$ as the intermediate galaxies. The results are shown in Fig. 10. The intermediate fraction in the standard model is increased by this change, and then it becomes comparable with the observation in the outer regions. At the central part of the cluster, however, this fraction is hardly changed and it is still too small.

In the ram-pressure model (lower panel), the increase of the intermediate fraction is more remarkable around $0.5R_{200}$. It is because that small threshold B/T value between disk-dominated class and intermediate class can reflect the small increase in B/T ratio by the ram-pressure stripping.

Interestingly, the intermediate fractions at the central part of the cluster have almost the same value in all cases. That is, the intermediate fraction at the cluster center is hardly affected by either the change of B/T criterion or the existence of the ram-pressure stripping. The reason is considered as follows. According to Okamoto & Nagashima (2001), galaxies in the central part of clusters typically separate into two types, i.e. almost pure disk galaxies and almost pure bulge galaxies, under the morphological evolution model only by major mergers. Eventually, ram-pressure stripping cannot affect the morphology of such pure disk or bulge systems, because the B/T ratios are not changed even if their disks are faded by the ram-pressure stripping. Okamoto & Nagashima (2001) have suggested that the intermediate fraction at the cluster center is always too small independent of the value of f_{bulge} and morphological thresholds in B/T classification.

Our conclusion is that we need additional mechanisms other than the ram-pressure stripping as the processes that directly change the morphology of disk-dominated galaxies into intermediate galaxies.

5. DISCUSSION

In this paper, we show the method to incorporate the ram-pressure stripping in a galaxy formation model that connected with cosmological N -body simulations. This method enables us to investigate effects of ram-pressure stripping in a fully cosmological context, namely, we can examine the effects following both the cluster and galaxies evolution. We have separately treated the stripping of diffuse hot gas confined in dark halos and stripping of cold gas in galactic disks by ram-pressure from an ICM. By this treatment, we clarify the effects of the ram-pressure stripping.

First of all we have examined effects of the hot gas stripping and confirmed the conclusion of previous studies using phenomenological models by comparing our model galaxies with CNOC sample. That is, observed color and SFR gradients in cluster galaxies arise naturally in hierarchical clustering by relatively slow truncation of star formation after they accrete on larger objects (Balogh, Navarro, & Morris 2000; Kodama &

Bower 2001; Diaferio et al. 2001). Such truncation is caused by the hot gas stripping in our model. After a galaxy fall into clusters star formation is gradually terminated in its star formation time-scale (~ 3 Gyr), because there is no supply of fresh cold gas from the hot gas reservoir.

By comparison of the galaxy population in the standard and ram-pressure models, we find that the role of the ram-pressure stripping of cold gas is quite small. This is because that star formation in cluster galaxies is sufficiently suppressed only by the hot gas stripping, therefore the amount of the cold gas remaining in the galaxies is very small when the cold gas is stripped by the ram-pressure. As a result, the effects of the ram-pressure stripping become negligible compared with observational errors.

Our model without the ram-pressure stripping is also successful in explaining the observed distribution of the bulge-dominated galaxies as a function of clustercentric radius. This result suggests that the formation model of bulges by major mergers gives good explanation to the formation of bulge-dominated population in clusters. On the other hand, this model produces much smaller fraction of intermediate galaxies in the cluster comparing with CNOC sample. Above results are perfectly consistent with the previous studies (Okamoto & Nagashima 2001; Diaferio et al. 2001). Our major interest is whether this deficiency of the intermediate population can be solved by including the ram-pressure stripping in our model. The results are follows. While the bulge-dominated and intermediate fractions are slightly increased by the ram-pressure stripping and these fractions show better agreement with the observation, these changes are quite small and the deficiency of the intermediate population still exists.

The problem on the morphological evolution model by major mergers is that galaxies in the very high-density regions typically separate into two morphological types, almost pure bulge and almost pure disk galaxies, as discussed by Okamoto & Nagashima (2001). The suppression of the star formation cannot changes the morphologies of such one-component systems. We then conclude that we should consider other morphological evolution mechanisms that change the morphology of the disk-dominated galaxies directly into the intermediate galaxy type. The cumulative accretion of small satellites (Walker, Mihos, & Hernquist 1996), the merger of the spiral galaxies with intermediate mass ratio (Bekki 1998), and the galaxy harassment (Moore et al. 1996, 1998, 1999) are promising mechanisms to match the intermediate galaxy fraction with the observed one.

We conclude that the influence of the ram-pressure stripping of disk cold gas on the properties of cluster galaxies is quite small and the hot gas stripping is the most important process to understand galaxy population in clusters. The ram-pressure stripping would play an important role if we adopted much longer star formation time-scale. However, such star formation time-scale cannot reproduce the observed cold gas content in the local galaxies.

In this paper we have discussed the effects of gas stripping on cluster galaxies by comparing the radial gradients in the simulated cluster with the observations rather than the redshift evolution of the cluster galaxies. We plan to investigate the redshift evolution of cluster galaxies including some morphological evolution model that are not treated here in due course.

We are grateful to S. Mineshige, Y. Fujita, and T. Kodama for their fruitful comments. Numerical computation in this work

was carried out on SGI Origin 2000 at Division of Physics, Graduate School of Science, Hokkaido University and on SGI

Origin 3000 at Yukawa Institute Computer Facility.

REFERENCES

- Abadi, M. G., Moore, B., & Bower, R. G. 1999, *MNRAS*, 308, 947
 Abraham, R. G. et al. 1996, *ApJ*, 471, 694
 Balogh, M. L., Schade, D., Morris, S. L., Yee, H. K. C., Carlberg, R. G., & Ellingson, E. 1998, *ApJ*, 504, 75
 Balogh, M. L., Morris, S. L., Yee, H. K.C., Carlberg, R. G., & Ellingson, E. 1999, *ApJ*, 527, 54
 Balogh, M. L., Navarro, J. F., & Morris, S. L. 2000, *ApJ*, 540, 113
 Barnes, J. E. 1996, in *ASP Conference Series 92, Formation of the Galactic Halo—Inside and Out*, ed. H. L. Morrison & A. Salajedini (San Francisco: ASP), 415
 Baugh, C. M., Cole, S., & Frenk, C. S. 1996, *MNRAS*, 283, 1361
 Bond, J. R., Cole, S., Efstathiou, G., & Kaiser, N. 1991, *ApJ*, 379, 440
 Binney, J., & Tremaine, S. 1987, *Galactic Dynamics*, (Princeton: Princeton Univ. Press)
 Benson, A. J., Cole, S., Frenk, C. S., Baugh, C. M., & Lacey, C. G. 2000, *MNRAS*, 311, 793
 Blanton, M., Cen, R., Ostriker, J. P., & Strauss, M. 1999, *ApJ*, 522, 590
 Bond, J. R., Cole, S., Efstathiou, G., & Kaiser, N. 1991, *ApJ*, 379, 440
 Bower, R. G. 1991, *MNRAS*, 248, 332
 Bower, R. G., Lucy, J. R., & Ellis, R. S. 1992, *MNRAS*, 254, 601
 Briel, U. G., Henry, J. P., & Böhringer, H. 1992, *MNRAS*, 259, L31
 Butcher, H. & Oemler, A. 1978, *ApJ*, 219, 18
 Butcher, H. & Oemler, A. 1984, *ApJ*, 285, 426
 Cen, R. & Ostriker, J. P. *ApJ*, 538, 83
 Cole, S., Aragón-Salamanca, A., Frenk, C. S., Navarro, J. F., & Zepf, S. E. 1994, *MNRAS*, 271, 781
 Cole, S., Lacey, C. G., Baugh, C. M., & Frenk, C. S. 2000 *MNRAS*, 319, 168
 Carlberg, R. G., Yee, H. K. C., & Ellingson, E. 1997, *ApJ*, 478, 462
 Couch, W. J., Barger, A. J., Smail, I. Ellis R. S., & Sharples, R. M. 1998, *ApJ*, 497, 188
 Davis, M., Efstathiou, G., Frenk, C. S., & White, S. D. M. 1985, *ApJ*, 292, 371
 Diaferio, A., Kauffmann, G., Balogh, M. L., White, S. D. M., Schade, D., & Ellingson, E. 2001, *MNRAS*, 323, 999
 Dressler A. 1980, *ApJ*, 236, 351
 Dressler A. et al. 1997, *ApJ*, 490, 577
 Ellingson, E., Lin, H., Yee, H. K. C., & Carlberg, R. G. 2001, *ApJ*, 547, 609
 Folkes, S. et al. 1999, *MNRAS*, 308, 459
 Fujita, Y., & Nagashima, M., 1999, *ApJ*, 516, 619
 Gallagher, J. S., Bushouse, H., & Hunter, D. A. 1989, *AJ*, 97, 700
 Ghigna, S., Moore, B., Governato, F., Lake, G., Quinn, T., & Stadel, J. 1998, *MNRAS*, 300, 146
 Gottlöber, S., Klypin, A., & Kravtsov, A. V. 2001, *ApJ*, 546, 223
 Governato, F., Moore, B., Cen, R., Stadel, J., Lake, G., & Quinn T. 1997, *New Astron.*, 2, 91
 Gunn, J. E., & Gott, J. R. 1972, *ApJ*, 176, 1
 Hoffman, Y., & Ribak, E. 1991, *ApJ*, 380, L5
 Huchtmeier, W. K., & Richter O.-G. 1988, *A&A*, 208, 237
 Katz, N., Hernquist, L., & Weinberg, D. H. 1999, *ApJ*, 523, 463
 Kauffmann, G. 1996, *MNRAS*, 281, 487
 Kauffmann, G., & Charlot, S. 1998, *MNRAS*, 294, 705
 Kauffmann, G., Colberg, J. M., Diaferio, A., & White, S. D. M. 1999, *MNRAS*, 307, 529
 Kauffmann, G., & Haehnelt, M. 2000, *MNRAS*, 311, 576
 Kauffmann, G., White, S. D. M., & Guiderdoni, B. 1993, *MNRAS*, 264, 201
 Kodama, T., & Bower, R. G. 2001, *MNRAS*, 321, 18
 Kodama, T., & Arimoto, N. 1997, *A&A*, 320, 41
 Kodama, T., Arimoto, N., Barger, A. J., & Aragón-Salamanca, A. 1998, *A&A*, 334, 99.
 Lacey, C., & Cole, S. 1993, *MNRAS*, 262, 627
 Larson, R. B., Tinsley, B. M., & Caldwell, C. N. 1980, *ApJ*, 237, 692
 Loverdy J., Peterson, B., Efstathiou, G., & Maddox, S. 1992 *ApJ*, 390, 338
 Moore, B., Katz, N., Lake, G., Dressler, A., & Oemler, A., 1996, *Nature*, 379, 613
 Moore, B., Lake, G., & Katz, N. 1998, *ApJ*, 495, 139
 Moore, G., Lake, G., Quinn, T., & Stadel, J. 1999, *MNRAS*, 304, 465
 Nagashima, M., & Gouda, N. 2001, *MNRAS*, 325, L13
 Nagashima, M., Totani, T., Gouda, N., & Yoshii, Y. 2001, *ApJ*, 557, 505
 Navarro, J. F., Frenk, C. S., & White, S. D. M. 1997, *ApJ*, 490, 493 (NFW)
 Okamoto, T., & Habe, A. 1999, *ApJ*, 516, 591
 Okamoto, T., & Habe, A. 2000, *PASJ*, 52, 457
 Okamoto, T., & Nagashima, M. 2001, *ApJ*, 547, 109
 Pearce et al. 1999, *ApJ*, 521, L99
 Press, W. H., & Schechter, P. L. 1974, *ApJ*, 187, 425
 Ratcliffe, A., Shanks, T., Parker, Q., & Fong, R. 1998, *MNRAS*, 293, 197
 Roukema, B. F., Peterson, B. A., Quinn, P. J., & Rocca-Volmerrange, B. 1997, *MNRAS*, 292, 835
 Salpeter, E. E. 1955, *ApJ*, 121, 161
 Sandage, A., Binggeli, B., & Tammann, G. A. 1985, *AJ*, 90, 1759
 Simien, F., & de Vaucouleurs, G. 1986, *ApJ*, 302, 564.
 Somerville, R. S., & Primack, J. R. 1999, *MNRAS*, 310, 1087
 Somerville, R. S., Primack, J. R., & Faber, S. M. 2001, *MNRAS*, 320, 504
 Springel, V., White, S. D. M., Tormen, G., & Kauffmann, G. 2000, preprint (astro-ph/0012055)
 Steinmetz, M. & Müller, E. 1995, *MNRAS*, 276, 549
 Sutherland, R., & Dopita, M. A. 1993, *ApJS*, 88, 253
 Terlevich, A. I., Caldwell, N., & Bower, R. G. 2001, preprint (astro-ph/0106337)
 Tormen, G. 1997, *MNRAS*, 290, 411
 van Dokkum, P. G., Franx, M., Kelson, D. D., Illingworth, G. D., Fisher, D., & Fabricant, D. 1998, *ApJ*, 500, 714
 Walker, I. R., Mihos, J. C., & Hernquist, L. 1996, *ApJ*, 460, 121
 Weinberg, D. H., Hernquist, L., Katz, N. 1997, *ApJ*, 477, 8
 Whitmore, B. C., Gilmore, D. M., & Jones, C. 1993, *ApJ*, 407, 489
 Yee, H. K. C., Ellingson, E., & Carlberg, R. G., 1996, *ApJS*, 102, 269
 Zucca E. et al. 1997, *A&A*, 326, 477

TABLE 1
PARAMETERS OF SIMULATIONS

Simulation	Constraint	N_h	N_l	ϵ_h	ϵ_l	m_h	m_l	R_{sim}	M_{target}
Field	None	636008	824438	5	20	5.5×10^8	4.4×10^9	20	1.87×10^3
Cluster	3σ peak	1121534	95406	5	50	5.5×10^8	3.5×10^{10}	22.5	5.23×10^4

Note. — Subscripts h and l indicate high-resolution and low-resolution particles, respectively. a length unit is h^{-1} Mpc and a mass unit is $h^{-1} M_{\odot}$

TABLE 2
PARAMETERS OF GALAXY FORMATION MODEL

$V_{\text{hot}} \text{ (km s}^{-1}\text{)}$	α_{hot}	$\tau_{*}^0 \text{ (Gyr)}$	α_{*}	f_{bulge}	$y \text{ (} Z_{\odot}\text{)}$
200	2.0	2.0	-1.3	0.2	3.0

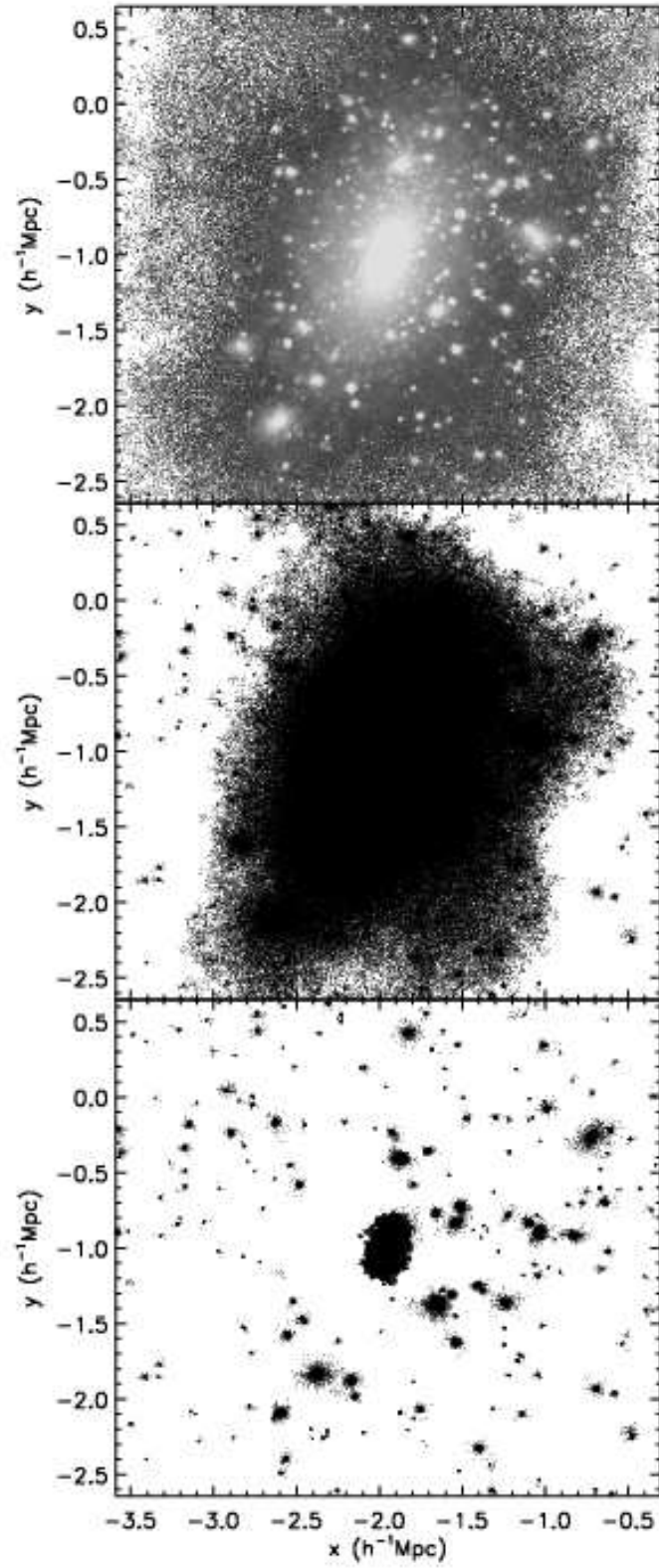


FIG. 1.— Density map (*top panel*), the x - y projection of the particles contained in FOF-halos (*middle panel*), and projection of those in SKID-halos (*bottom panel*) within cluster's virial radius at $z = 0$.

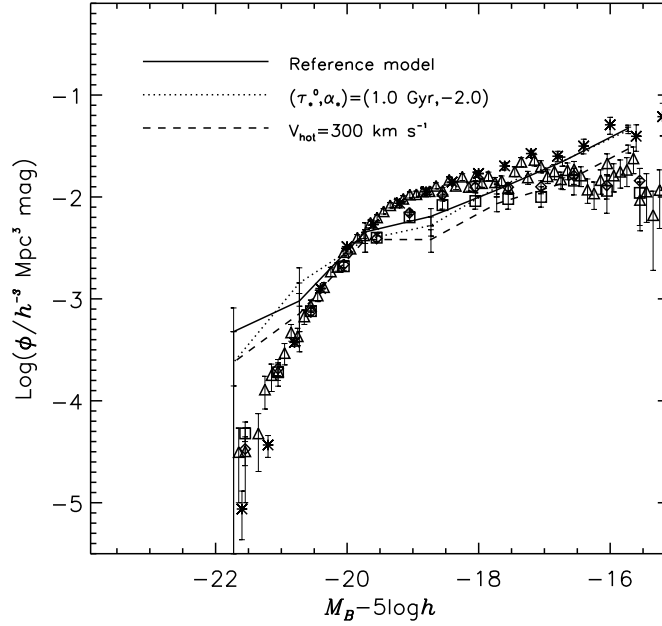


FIG. 2.— B -band luminosity functions in the field model. Squares, asterisks, diamonds, and triangles indicate observed luminosity functions taken from APM, ESP, UKST, and 2dF, respectively. The luminosity function by the reference model is represented by the solid line. The luminosity functions with $(\tau_*^0/\text{Gyr}, \alpha_*) = (1.0, -2.0)$ and with $V_{\text{hot}} = 300 \text{ km s}^{-1}$ are indicated by the dotted and dashed lines, respectively.

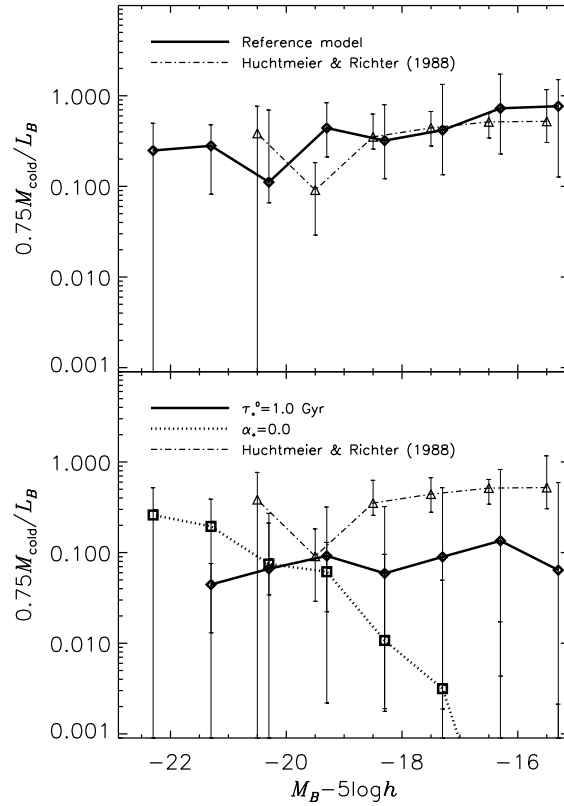


FIG. 3.— The cold gas content of spiral and irregular galaxies as a function of luminosity. In each panel the dot-dashed line shows observational estimate of the median of the distribution of the M_{H_I}/L_B by (Huchtmeier & Richter 1988). In upper panel, the thick solid line indicates the cold hydrogen fraction, $0.75M_{\text{cold}}/L_B$, of our galaxies with $T \geq 1$ in the reference model. In lower panel, the models with $\tau_*^0 = 1.0 \text{ Gyr}$ and $\alpha_* = 0.0$ are represented by the thick solid and dotted lines, respectively. The error bars show the 25th to 75th percentile of the distribution. There are some bins that contain only one or two galaxies at the bright end, we then attach the error bars by the simple $1/\sqrt{n}$ method to these points.

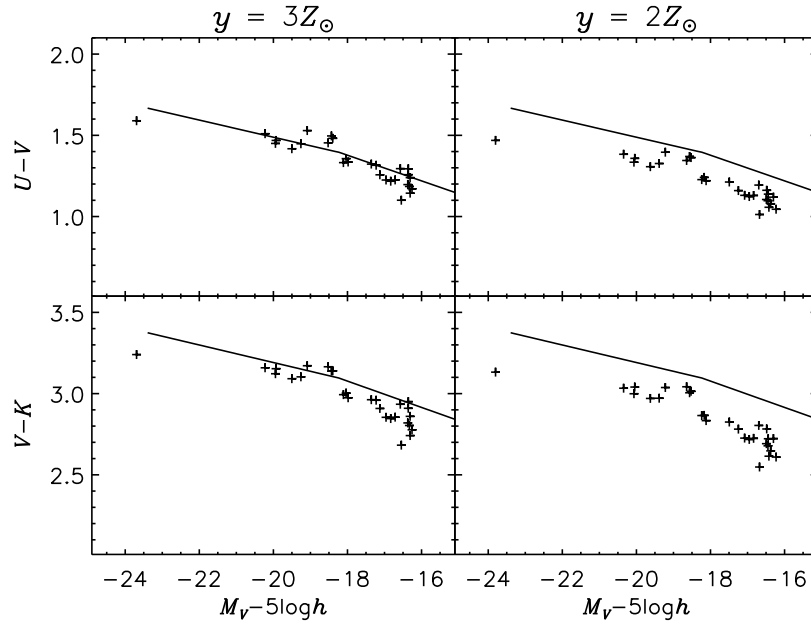


FIG. 4.— Color-magnitude diagrams for the ellipticals within cluster's core in the standard model at $z=0$. Left: Upper and lower panels show M_V v.s. $U-V$ and M_V v.s. $V-K$, respectively, for the model with $y=3Z_\odot$ (reference model). Right: Same as the left panels but for the model with $y=2Z_\odot$. The solid lines show the observed color-magnitude relation for cluster ellipticals by Bower, Lucy, & Ellis (1992), which are applied aperture correction (Kodama et al. 1998).

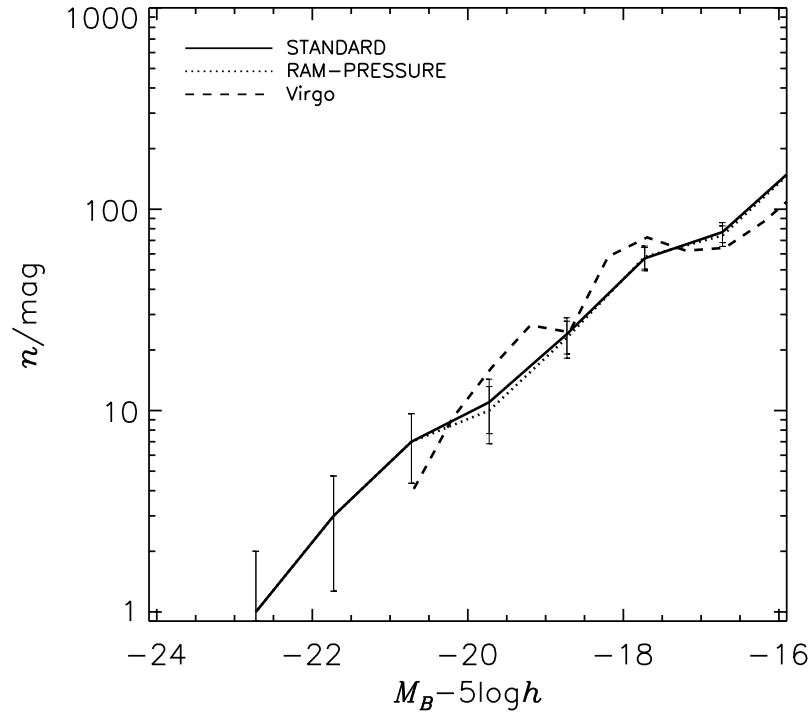


FIG. 5.— B -band luminosity functions of cluster galaxies. The solid and dotted lines indicate the luminosity functions of the standard model and the ram-pressure model, respectively. The dashed line is the luminosity function of the Virgo cluster galaxies by Sandage, Binggeli, & Tammann (1985).

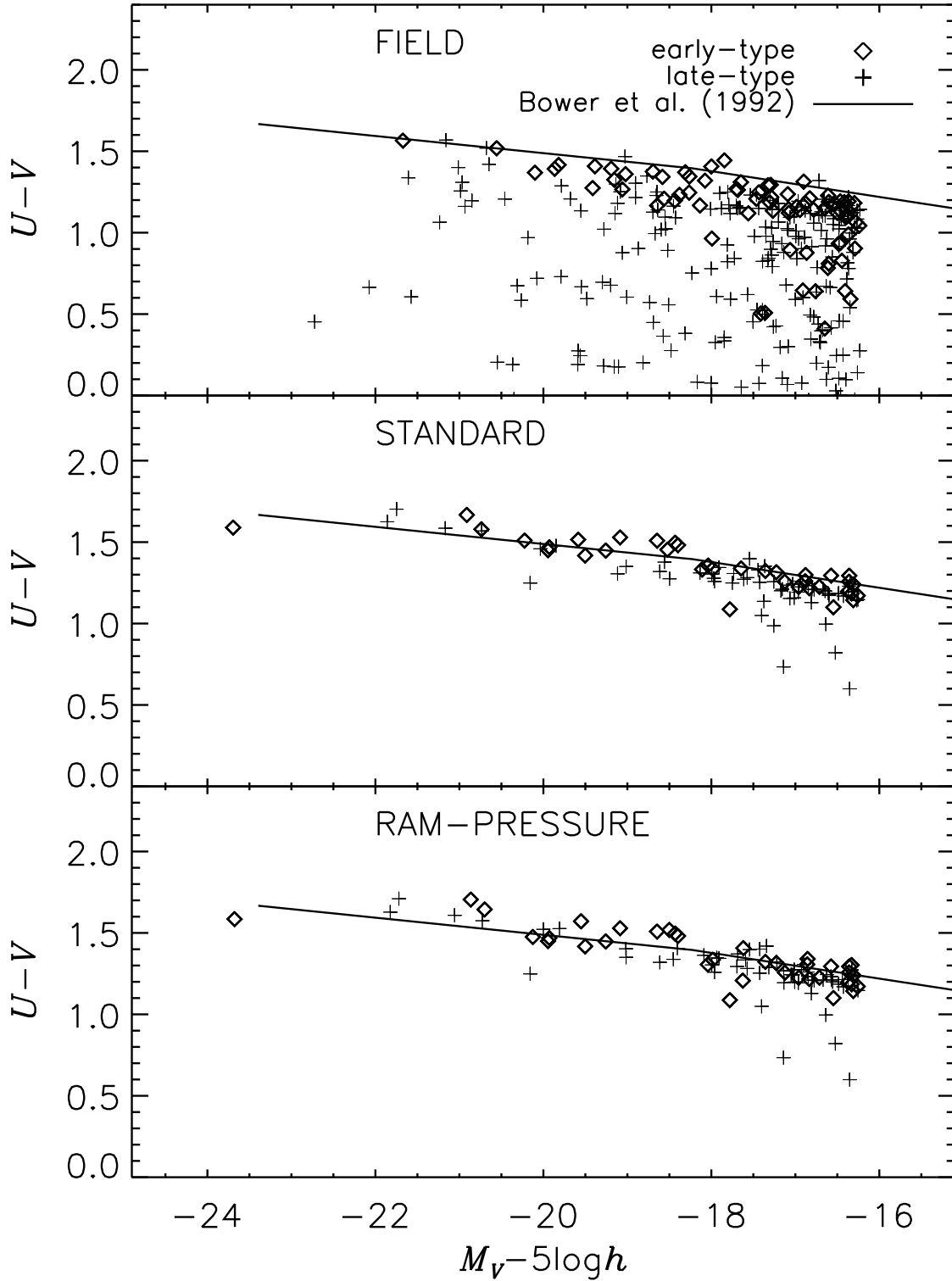


FIG. 6.— Color-magnitude diagrams at $z=0$. We show $U-V$ colors of galaxies in the field model (*top panel*) and galaxies within clusters' core in the standard (*middle panel*) and ram-pressure (*bottom panel*) models as a function of V -band luminosity. Galaxies with $T < 0.92$ by eq. (8) are classified as early-type galaxies (diamonds) and other galaxies are classified as late-type galaxies (pluses). The solid lines show the observed color-magnitude relation for cluster ellipticals by Bower, Lucy, & Ellis (1992), which are applied aperture correction (Kodama et al. 1998).

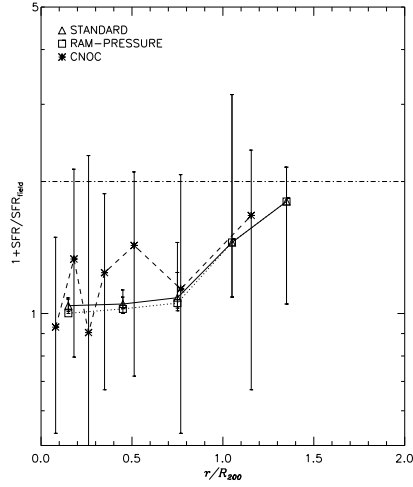


FIG. 7.— The SFRs of galaxies with $M_R < -20.5$ are plotted as a function of projected radius at $z = 0.2$. The SFRs have been scaled by dividing by the median SFR of field galaxies at the same magnitude and redshift, and they are added 1. The triangles and squares indicate the median SFRs in the standard model and in the ram-pressure model, respectively. The observed SFRs of the galaxies in the CNOC sample are taken from Diaferio et al. (2001) and shown by the asterisks. The dot-dashed line indicates the median SFR in the field model. An error bar shows the 25th to 75th percentile of the distribution in each bin.

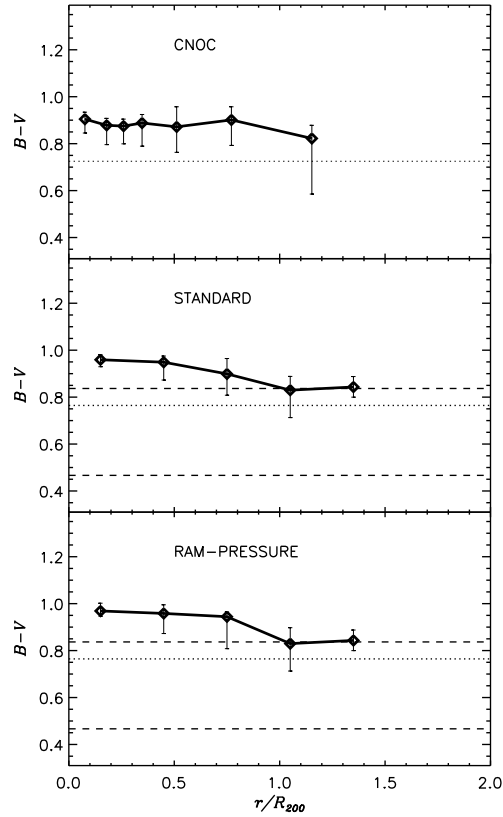


FIG. 8.— The rest frame $B-V$ colors of cluster galaxies with $M_R < -20.5$ are plotted as a function of projected radius. In the top panel, the diamonds denote the observed median colors of the CNOC sample, which are taken from Diaferio et al. (2001). The median color of field galaxies with $M_R < -20.5$ at the same redshift range are shown by the dotted line. In the middle panel and the bottom panel we show the median colors at $z = 0.2$ by the standard model and ram-pressure model, respectively. The median color of the galaxies in the field model with $M_R < -20.5$ at $z = 0.2$ is shown by the dotted line in each panel. An error bar shows the 25th to 75th percentile of the distribution in each bin. We also show the 25th to 75th percentile of the distribution for the galaxies in the field model by the dashed lines.

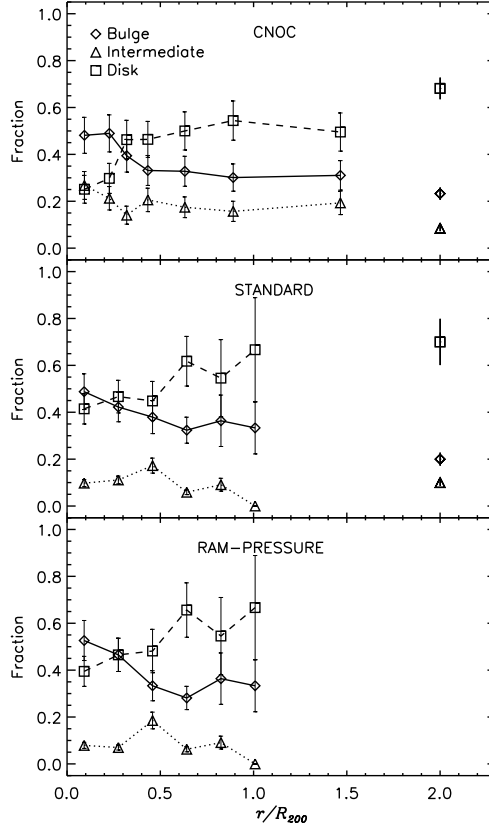


FIG. 9.— The morphological fractions are plotted as a function of projected radius. The diamonds, triangles, and squares indicate the bulge-dominated, intermediate, and disc-dominated type galaxies, respectively. In the top panel we show the observed fractions for the galaxies with $M_R < -20.5$ in the CNOC sample, which are taken from Diaferio et al. (2001). In the middle and bottom panels we show the morphological fractions obtained in the standard and ram-pressure models, respectively. The boundaries between the morphological classes are chosen so that the fractions in the field model match the fraction of the field galaxies in the CNOC sample. The symbols at $r/R_{200} = 2$ indicate the fractions in the field in each panel. The error bars present the Poisson errors.

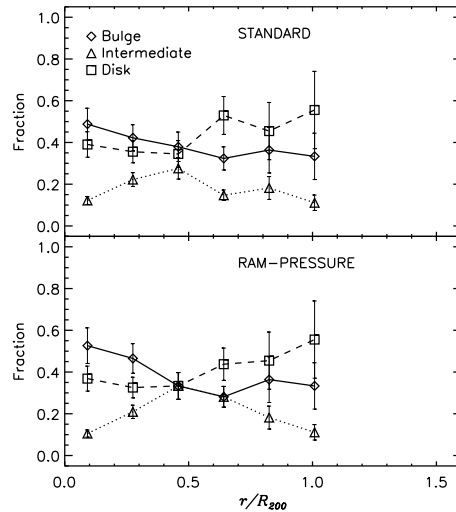


FIG. 10.— Same as Fig. 9 but for the classification for the intermediate class with $0.15 < B/T < 0.4$. We show the morphological fractions in the standard model and ram-pressure model in the upper panel and lower panel, respectively.